Tuning the magnetic and magnetocaloric properties of austenitic *Ni-Mn-*(*In,Sn*) Heuslers

G. Cavazzini[a,b], F. Cugini[a,b,*], M. E. Gruner[c], C. Bennati[b], L. Righi[d,b], S. Fabbrici[b], F. Albertini[b] and M. Solzi[a,b]

[a] *Department of Mathematical, Physical and Computer Sciences, University of Parma, Parco Area delle Scienze 7/A 43124 Parma, Italia.*
[b] *IMEM-CNR Institute, Parco Area delle Scienze 37/A 43124 Parma, Italia.*
[c] *Department of Physics and Center for Nanointegration, CENIDE, University of Duisburg-Essen, Lotharstr. 1, 47048 Duisburg, Germany.*
[d] *Department of Chemistry, Life Sciences and Environmental Sustainability, University of Parma, Parco Area delle Scienze 17/A 43124 Parma, Italia.*

Abstract

In this work, it is highlighted the occurrence of different physical mechanisms that independently control the saturation magnetization and the ferro-paramagnetic transition temperature of Ni-Mn-based Heusler compounds, opening new possibilities in mastering the functional properties of this wide class of magnetic materials. The magnetic, structural and magnetocaloric features of a complete $Ni_{48}Mn_{36}In_{16-x}Sn_x$ (x= 0-16) series are presented. The observed different trends of the critical temperature and of the saturation magnetization on varying the Sn to In ratio are discussed on the basis of results obtained from first-principles calculations of the electronic structure and the magnetic interactions of the compound.

Keywords: Heusler compounds, magnetocaloric, energy conversion, intermetallic compounds, first-principles calculations

* Corresponding author e-mail: francesco.cugini@unipr.it

Thermo-magnetic energy conversion devices are heat engines and heat pumps that transform thermal and mechanical energy by exploiting the magnetic properties of materials. They can be used to convert wasted thermal energy in mechanical or electrical energy for the harvesting of heat dissipated from low-temperature heat sources (T<80°C) [1,2]. They can also be exploited as a promising efficient and eco-friendly alternative to replace the current gas-compression-based technology of refrigeration [3]. The magnetic refrigeration is based on the magnetocaloric effect (MCE), consisting in a temperature change (ΔT_{ad}) or an entropy change (Δs_T) induced in a magnetic material by a magnetic field variation under adiabatic or isothermal conditions, respectively [4]. The thermo-magnetic energy conversion requires materials featured by a large temperature variation of magnetization ($\partial M(T,H)/\partial T$). This condition is mainly fulfilled at magnetic phase transitions. First-order magnetic phase transitions have been intensively investigated, during the last decades, thanks to the large values of magnetization change with temperature and to the possibility to obtain a giant-MCE (GMCE) due to the contribution of the latent heat [5,6]. However, their intrinsic irreversibility reduces the efficiency of thermomagnetic cycles. Moreover, the variations of volume and crystal symmetry, often associated to these transformations, can introduce issues of structural fatigue and a degradation of performance during continuous transformation cycles. Instead, second-order transitions show fully reversible effects and limited mechanical drawbacks [7].

Ni-Mn-based Heusler compounds represent an interesting class of materials for thermo-magnetic energy conversion applications. Their structure allows, by changing the composition, the tuning over a large temperature range of both a second-order and a first-order magnetic transition [8-10]. The first-order transition, from the cubic austenite to a low-symmetry phase (martensite), can originate a large inverse MCE [5,11]. Alternatively, the second-order ferro-paramagnetic transition of the austenitic phase can be suitably exploited in thermo-magnetic devices [7]. In this case, two handles can be adjusted to optimize the performances of the material: the saturation magnetization (M_s) and the critical temperature (T_c). The ferromagnetic state of austenite results from the interaction between Mn and Ni magnetic moments and it can be enhanced by

increasing the Mn content at the expense of the Z element ($Ni_{50}Mn_{25+x}Z_{25-x}$). The almost linear increase of magnetization with *x* is limited by the concurrent increase of the temperature of the first-order martensitic transition that can suppress the ferro-paramagnetic transition of austenite [9,10]. Concerning the control of the critical temperature, it seems mainly related to the Z element, and less dependent on the Mn/Z ratio [9,10,12]. Besides the chemical composition, the magnetic properties of this class of compounds are dependent also on microstructural features and on the degree of atomic order [13-17].

The independent control of both the ferro-paramagnetic transition and the saturation magnetization represents an important tool to optimize the materials properties for their application in technological devices. However, a clear understanding of the features which define the magnetic configuration of these compounds has not yet achieved.

In order to establish the fundamental factors determining the critical temperature and the saturation magnetization in Ni-Mn-based Heuslers and their impact on their magnetocaloric properties, we studied a series of $Ni_{48}Mn_{36}In_{16-x}Sn_x$ ($0 \leq x \leq 16$) compounds by comparing structural, magnetic and magnetocaloric experimental results with information derived from first-principles calculations.

A series of polycrystalline compounds with nominal composition $Ni_{48}Mn_{36}In_{16-x}Sn_x$ (x =0, 2, 4, 6, 8, 10, 12, 14, 16; named: Sn0, …, Sn16) were prepared by arc-melting high-purity (99.99 wt.%) elements under a protective argon atmosphere. To homogenize the sample two different annealing treatments, followed by water quenching, were used: 3 days at 1073 K for $0 \leq x \leq 8$; 1 day at 1173 for $x > 8$ [18, 19]. The composition of the compounds (reported in the S.M., Table S.1) was determined by energy dispersive spectroscopy (EDS). The structural characterization was carried out by X-ray powder diffraction using Cu-Kα radiation, with a Thermo ARL X'tra diffractometer. The magnetic measurements were performed by using a Superconducting Quantum Interference Device (SQUID) MPMS-XL magnetometer (Quantum Design). The direct adiabatic temperature change data were obtained with a purpose-built probe, based on a Cernox bare chip resistive temperature sensor, by applying a magnetic field change of 1 T [20].

The X-rays diffraction patterns, collected at room temperature, confirmed the $L2_1$ structure of the austenitic phase for all the compounds. There is no evidence of secondary phases or compositional inhomogeneities. The lattice parameter (*a*), determined through Le Bail refinement, shows a very little decrease as the Sn concentration increases (< 0.2% in the whole series, Fig. 1.a). This result agrees with the data reported by S. Dwevedi and B. Tiwari [21] for the Heusler compounds with nominal composition $Ni_{50}Mn_{34}In_{16}$ and $Ni_{50}Mn_{34}In_8Sn_8$. A similar trend with In to Sn ratio was obtained also for $Pd_{50}Mn_{25}(In_{1-x}Sn_x)_{25}$ compounds [22].

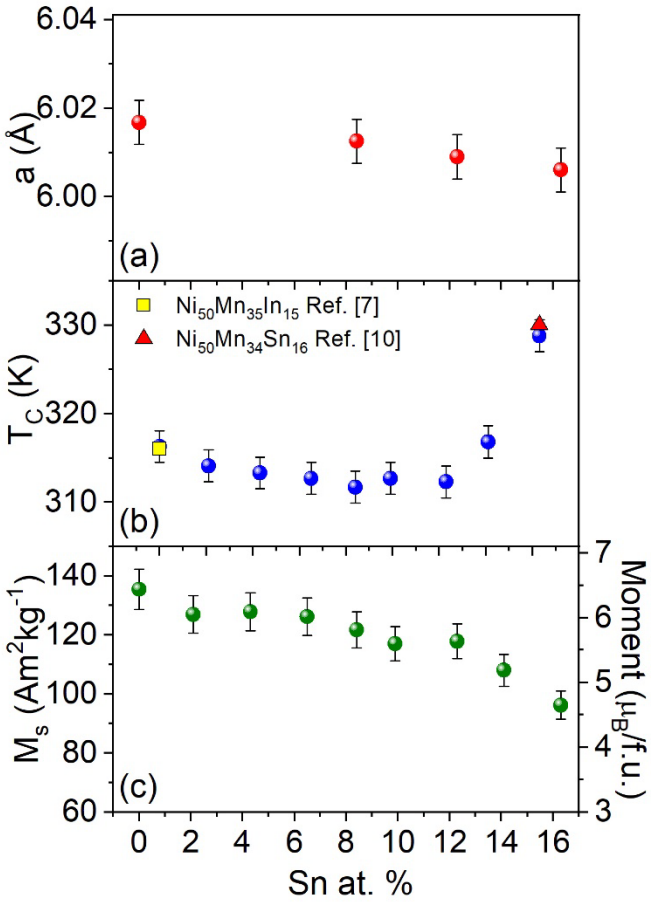

Fig.1*: Dependence of the lattice constant (a), of the critical temperature (b) and of the saturation magnetization (c) on the Sn at. % content. The error bars of T_c and M_s were obtained as the standard deviation by measuring different fragments of the same sample.*

The temperature dependence of low-field magnetization has been measured from 5 K to 380 K. All the compounds display a ferromagnetic austenitic phase stable down to 5 K, with the ferro-paramagnetic transition just above room temperature (Table 1, *M(T)*

curves are reported in S.M. Fig. S.1). Fig. 1.b reports the change of the critical temperature as a function of the Sn content. Two opposite behaviours are evident: from Sn0 to Sn8, the magnetic transition temperature gradually lowers; by contrast, increasing the Sn concentration from Sn8 to Sn16, the transition moves to higher temperatures. The T_c values of the endmembers of the series agree with those reported in prior published works with similar compositions: $Ni_{50}Mn_{34}In_{16}$ ($T_c \approx 316$ *K)* and $Ni_{49.6}Mn_{34.2}Sn_{16.1}$ ($T_c \approx 330$ *K*) [7, 10].

	M_s- (Am^2kg^{-1})	T_c (K)	$\lvert\Delta s_T^{max}\rvert$ ($JKg^{-1}K^{-1}$)	ΔT_{ad}^{max} (K)
Sn0	135.5 ± 6.8	316.3 ± 1.8	2.07 ± 0.11	0.98 ± 0.07
Sn2	127.0 ± 6.4	314.1 ± 1.8	-	0.89 ± 0.07
Sn4	127.9 ± 6.4	313.3 ± 1.8	1.81 ± 0.10	0.85 ± 0.07
Sn6	126.2 ± 6.3	312.7 ± 1.8	-	0.77 ± 0.07
Sn8	121.7 ± 6.1	311.7 ± 1.8	1.57 ± 0.10	0.74 ± 0.07
Sn10	117.1 ± 5.9	312.7 ± 1.8	-	0.65 ± 0.07
Sn12	117.8 ± 5.9	312.3 ± 1.8	1.43 ± 0.09	0.71 ± 0.07
Sn14	108.0 ± 5.40	316.8 ± 1.8	1.2 ± 0.09	0.68 ± 0.07
Sn16	96.2 ± 4.8	328.8 ± 1.8	1.12 ± 0.07	0.53 ± 0.07

Table 1*: Schematic summary of the experimental values of the saturation magnetization (M_s), the critical Temperature (T_c) and the MCE quantities ($\lvert\Delta s_T^{max}\rvert$, ΔT_{ad}^{max}) for a $\mu_0\Delta H = 1.0$ T.*

The saturation magnetization was estimated by measuring the magnetization of the compounds at 5 K under an applied magnetic field of 2 T, where the magnetization is almost fully saturated [7,9,14] due to the very low coercivity and magnetocrystalline anisotropy of these alloys. The approximated saturation magnetization values reported in table 1 agree within the experimental error with the spontaneous magnetization values that can be estimated by Arrot plots, as further described in the supplementary materials. Differently from T_c, the saturation magnetization, reported in Fig. 1.c and Table 1, continuously decreases with the increment of Sn concentration. A 30% decrease of M_s was obtained between the $Ni_{48}Mn_{36}In_{16}$ and the $Ni_{48}Mn_{36}Sn_{16}$ samples. The values of saturation magnetization measured for the Sn0 and Sn16 samples are slightly higher than those reported in literature for $Ni_{50}Mn_{34}In_{16}$ and $Ni_{49.6}Mn_{34.2}Sn_{16.1}$ samples [7, 10, 14]. Such a slight difference could be ascribed to the different Ni/Mn ratio.

The isothermal entropy change Δs_T was derived from iso-field *M(T)* measurements (reported in S.M., Fig. S.2) by applying the Maxwell relation [23]. In Fig. 2 the $\Delta s_T(T)$ for a $\mu_0 \Delta H$ of 1 T is shown for some selected samples. The peak values of the $\Delta s_T(T)$ curves are reported as a function of Sn concentration in the inset of Fig. 2: it clearly shows a gradual decrease of the Δs_T^{max} with the increase of Sn. The entropy change of the Sn16 sample is about 45% less with respect to that of In-sample (Sn0). The observed linear dependence of Δs_T^{max} on composition can be correlated with the analogous trend observed for M_s.

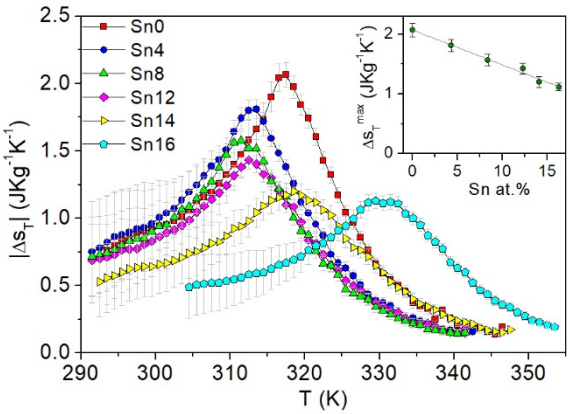

Fig. 2: *Isothermal entropy change as a function of temperature for selected samples, with a magnetic field variation $\mu_0 \Delta H$ = 1T. Inset: maximum Δs_T as a function of the Sn content.*

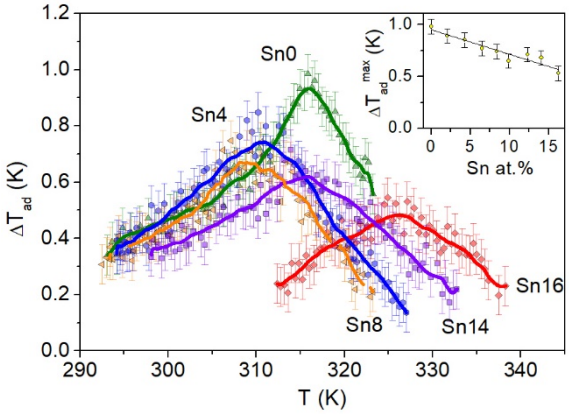

Fig. 3: *Adiabatic temperature change as a function of temperature for a magnetic field change $\mu_0 \Delta H$= 1T. Inset: maximum ΔT_{ad} as a function of the Sn content.*

Fig. 3 reports the adiabatic temperature change $\Delta T_{ad}(T)$, which is the other key quantity that characterizes the MCE. The ΔT_{ad} resulted completely reversible as expected in the case of second order transitions. The peak of ΔT_{ad} lowers linearly with the Sn content,

reaching a decrease of about 45% between Sn0 and Sn16 sample. The obtained values of the MCE for the Sn0 sample are quite in agreement with the results presented in Ref.s: [5,7,14]. Regarding the mixed In-Sn compositions, we obtained the same trend with Sn content of ΔT_{ad}^{max} and Δs_T^{max} as that reported in Ref. [24] for $Ni_{50}Mn_{34}(In,Sn)_{16}$ Heusler ribbons, while the absolute values of both the magnetocaloric parameters are superior thanks to the higher content of Mn that increases the values of M_s.

The main point of the obtained results is the presence of two different trends of variation of magnetic and magnetocaloric parameters with the Sn content. This leads to the hypothesis that different mechanisms exist, which separately control and influence the M_s and T_c, thus opening new possibilities to optimize and tune the MCE in these compounds. Indeed, while the saturation magnetization and the MCE (ΔT_{ad} and Δs_T) show a similar linear reduction with increasing the Sn amount, the critical temperature follows a nonmonotonic trend with composition. This fact cannot be simply related to a variation of the Mn-Mn distance conditioned by the change of the cell parameter with composition, which is indeed rather limited.

In order to figure out the causes of the observed T_c and M_s changes with the Sn/In ratio, one should consider the complex structure of magnetic interactions in Ni-Mn-based Heusler compounds. In these materials, the magnetic moments are mainly localized on the Mn atoms. However, all the Mn and Ni moments significantly contribute to the stabilization of the ferromagnetic state and to the determination of T_c, which results from the overlap of different Ni-Ni, Mn-Mn and Ni-Mn magnetic interactions. For the stoichiometric composition, the nearest Mn-Mn distances in the Mn sublattice (4a Wyckoff position) is rather large, impeding a significant direct exchange coupling between the Mn atoms and favouring indirect mechanisms mediated by the conduction electrons [25]. These mechanisms have been interpreted in terms of the RKKY model or Anderson's *s-d* mixing model, depending on the number of conduction *sp* electrons, the spin polarization and the position of the unoccupied Mn 3d states with respect to the Fermi level [26, 27]. In the case of Mn-rich Heusler compounds, with general stoichiometry $Ni_{50}Mn_{25+x}Z_{25-x}$, the excess Mn atoms occupy the Z (4b) site and give rise to a complex scenario of ferro- and antiferromagnetic interactions, either short or long

range, between Mn atoms belonging to different sublattices. Instead, the direct interaction between Ni (on the 8c site) and Mn atoms (on both the 4a and 4b sites) remains ferromagnetic [28]. The competition between all these different magnetic interactions makes the T_c of Ni-Mn based compounds not very sensitive to the changes in Ni/Mn ratio. This evidence of many experimental works was confirmed by first-principle calculations performed, for example, on off-stoichiometric Mn-rich $Ni_{50}Mn_{25+x}In_{25-x}$ [7] (Fig. 8 of Supplementary Materials) and $Ni_{50}Mn_{25+x}Sb_{25-x}$ compounds [16]. The weighted sum of all the different kinds of exchange interactions is indeed almost constant as a function of the Mn excess in the range corresponding to the austenitic phase. This fact justifies the absence of correlation between the measured T_c values and the Ni/Mn changes due to a slight random variation from the nominal compositions in the prepared samples. Instead, a strong dependence of magnetic properties of the studied compounds on the non-magnetic Z atom is evident. This result supports the interpretation of previous first-principles density functional theory (DFT) calculations that the conduction electrons of the non-magnetic atom play an important role in controlling the exchange interactions between Mn atoms [26, 29].

In order to verify this hypothesis, first-principles calculations of the Mn-rich mixed In-Sn compositions were performed (details are reported in S.M., Section 3). Two magnetic states were considered, a ferrimagnetic one, where the moments of the Mn atoms located on the 4b sites are reversed, and the entirely ferromagnetic solution. The latter turned out to be favoured for all compositions under consideration for the selected lattice constant (a = 6.012 Å). Fig. 4 shows the variation of magnetization (upper panel) and T_c (lower panel) for the ferro- and ferrimagnetic configurations of $L2_1$ austenite. For both cases, we see a minute decrease of the magnetic moment with increasing Sn-content by a few percent. This change arises essentially from the steady decrease in the Ni moments, while the moments on the Mn(4b) sites increase (in absolute numbers), which slightly enhances this trend for the ferrimagnetic state, where the Mn(4b) moments are reversed, but partially compensates it for the ferromagnet. The Mn(4a) moments decrease as well, but on a much smaller scale. These observations agree with previous first-principles calculations on stoichiometric compounds [26,29]. The

magnetization corresponding to the completely ferromagnetic arrangement fits the experimental value much better in the In-rich case. It is significantly larger, since a considerable fraction of Mn atoms on the 4b-sites are reversed in the ferrimagnetic case. Both show, however, only a slight variation with composition, which is much smaller than in the experiment (about 1.4% for the ferro- and 5.3% for the ferrimagnetic configuration instead of 34% of experimental results). A potential explanation for the much more pronounced decrease in experiment involves the presence of inhomogeneous magnetic configurations, i.e., mixed ferro- and ferrimagnetic domains, which effectively lower the magnetization and increase with Sn content. This might be expected as a consequence of compositional inhomogeneities or decomposition into stoichiometric and Mn-rich Heusler compositions, which has been discussed recently for the ternary Ni-Mn-In and Ni-Mn-Sn compounds [30].

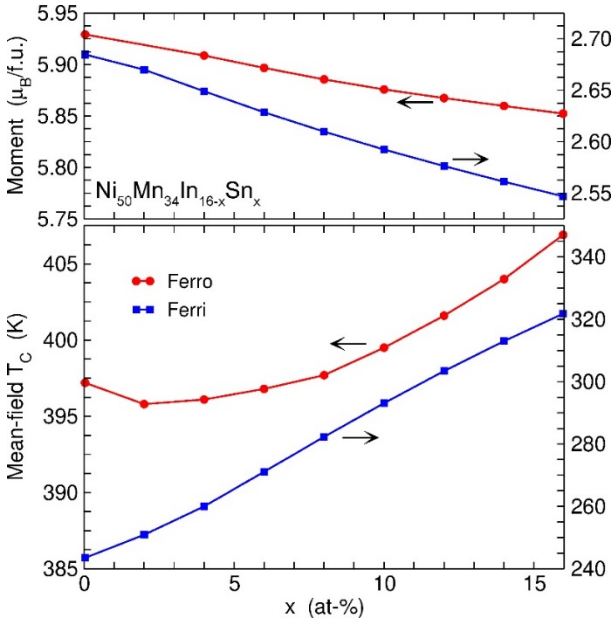

***Fig. 4**: Composition dependence of the magnetic moment per formula unit (upper panel) and ferro-paramagnetic critical Temperature, T_C, (lower panel) of $Ni_{50}Mn_{34}In_{16-x}Sn_x$ obtained from first-principles calculations for the ferromagnetic (red circles, left axis) and ferrimagnetic (blue squares, right axis) spin configurations. T_C is calculated from a Heisenberg-model with ab initio exchange parameters in the mean-field approximation, which typically overestimates the transition point by 20-30%.*

The transition temperature, however, is determined by the regions with the largest degree of magnetic order. Keeping in mind that the mean-field approximation

systematically overestimates the magnetic transition temperatures by 20-30%, the T_C of ferromagnetic configurations indeed match the experimental trend quite well. This indicates that the non-monotonous behaviour of T_C might be related to the intrinsic electronic properties of the ferromagnetic phase. In the spirit of the discussion above, we ascribe it to the delicate competition between the decrease in the near-neighbour Mn(4a)-Mn(4b) and Mn-Ni interactions with increasing Sn-content on the one hand, and, on the other, to the opposite trend exhibited by the longer-ranged RKKY-like contributions, such as the Mn(4a)-Mn(4a), which were pointed out to be relevant for the magnetic properties of similar Heusler systems earlier [16, 29, 31, 32].

In conclusions, we presented a structural, magnetic and magnetocaloric characterization of a complete series of $Ni_{48}Mn_{36}In_{16-x}Sn_x$ ($0 \leq x \leq 16$) Heusler compounds, together with the results of first-principles calculations. All the realized samples show a fully reversible MCE across the ferro-paramagnetic transition of the austenitic phase, which is stable down to 5 K. The transition temperature follows a non-monotonous trend with Sn content: it decreases with increasing Sn up to 8 at. %, while it abruptly rises. On the contrary, the saturation magnetization and the MCE linearly decrease with the Sn content. First-principles calculations suggest the intrinsic nature of the behaviour of the critical temperature of ferromagnetic austenite, which turns out to be strongly related to the electronic properties of the compound. On the contrary, the significant change of saturation magnetization might be justified by considering a mixed configuration of ferro- and ferrimagnetic domains.

Further calculations and experimental measurements, carried out by using local magnetic probes (e.g. neutron diffraction and solid state NMR), would be required to figure out the specific causes of magnetic parameters variation. Their deep understanding will contribute to a better control and optimization of the functional properties of Ni-Mn-based Heusler compounds. In particular, the possibility to independently tune the saturation magnetization and the critical temperature, suggested by the results of this work, is fundamental to exploit this class of materials in efficient thermomagnetic energy-conversion devices. Furthermore, from a practical point of view, this work stresses the chance to replace up to 50% of the critical element

In by the abundant and affordable Sn element, still maintaining a relevant magnetocaloric performance (reduced by only 20% with respect to In-compound).

Acknowledgments

This work has been supported by the FRIMAG project, funded by Emilia-Romagna region within the 2014-20 POR-FESR program (CUP E32F16000190007).
MEG gratefully acknowledges funding by the Deutsche Forschungsgemeinschaft via the priority program SPP 1599 (GR3498/3-2).

References

[1] R.A. Kishore, S. Priya, Renew. Sustain. Energy Rev. 81 (2018) 33-44.
[2] M. Gueltig, F. Wendler, H. Ossmer, M. Ohtsuka, H. Miki, T. Takagi, M. Kohl, Adv. Energy Mater. 7 (2017) 1601879.
[3] A. Kitanovski, J. Tušek, U. Tomc, U. Plaznik, M. Ožbolt, A. Poredoš, Magnetocaloric Energy Conversion From Theory to Applications, Springer I (2015).
[4] V.K. Pecharsky, K.A. Gschneidner, A.O. Pecharsky, A.M. Tishin, Phys. Rev. B 64 (2001) 144406.
[5] J. Liu, T. Gottschall, K.P. Skokov, J.D. Moore, O. Gutfleisch, Nat. Mater. 11 (2012) 620-625.
[6] V.K. Pecharsky, K.A. Gschneidner, Phys. Rev. Lett. 78 (1997) 4494-4497.
[7] S. Singh, L. Caron, S.W.D. Souza, T. Fichtner, G. Porcari, S. Fabbrici, C. Shekhar, S. Chadov, M. Solzi, C. Felser, Adv. Mater. 28 (2016) 3321-3325.
[8] F. Albertini, S. Fabbrici, A. Paoluzi, J. Kamarad, Z. Arnold, L. Righi, M. Solzi, G. Porcari, C. Pernechele, D. Serrate, P. Algarabel, Trans Tech Publ. 684 (2011) 151-163.
[9] T. Krenke, M. Acet, E.F. Wassermann, X. Moya, L. Mañosa, A. Planes, Phys. Rev. B 73 (2006) 174413.
[10] A. Çakır, L. Righi, F. Albertini, M. Acet, M. Farle, Acta Mater. 99 (2015) 140-149.
[11] S. Fabbrici, G. Porcari, F. Cugini, M. Solzi, J. Kamarad, Z. Arnold, R. Cabassi, F. Albertini, Entropy 16 (2014) 2201-2222.
[12] F. Albertini, M. Solzi, A. Paoluzi, L. Righi, Mater. Sci. Forum 583 (2008) 169-196.

[13] F. Cugini, G. Porcari, S. Fabbrici, F. Albertini, M. Solzi, Philos. Trans. R. Soc. A Math. Phys. Eng. Sci. 374 (2016) 2074.

[14] F. Cugini, L. Righi, L. van Eijck, E. Brück, M. Solzi, J. Alloys Compd. 749 (2018) 211-216.

[15] V. Recarte, J.I. Perez-Landazabal, V. Sanchez-Alarcos, J.A. Rodriguez-Velamazan, Acta Mater. 60 (2012) 1937-1945.

[16] V.D. Buchelnikov, P. Entel, S. V Taskaev, V. V Sokolovskiy, A. Hucht, M. Ogura, H. Akai, M.E. Gruner, S.K. Nayak, Phys. Rev. B 78 (2008) 184427.

[17] F. Cugini, G. Porcari, T. Rimoldi, D. Orsi, S. Fabbrici, F. Albertini, M. Solzi, JOM 69 (2017) 1422-1426.

[18] E. Wachtel, F. Henninger, B. Predel, J. Magn. Magn. Mater. 38 (1983) 305-315.

[19] T. Miyamoto, W. Ito, R.Y. Umetsu, R. Kainuma, T. Kanomata, K. Ishida, Scr. Mater. 62 (2010) 151-154.

[20] G. Porcari, M. Buzzi, F. Cugini, R. Pellicelli, C. Pernechele, L. Caron, E. Brück, M. Solzi, Rev. Sci. Instrum. 84 (2013) 073907.

[21] S. Dwevedi, B. Tiwari, J. Alloys Compd. 540 (2012) 16-20.

[22] P.J. Webster, M.R.I. Ramadan, J. Magn. Magn. Mater. 5 (1977) 51-59.

[23] V.K. Pecharsky, K.A. Gschneidner, J. Appl. Phys. 86 (1999) 565-575.

[24] F. Cugini, D. Orsi, E. Brück, M. Solzi, Appl. Phys. Letters 113 (2018) 232405.

[25] J. Kübler, A.R. William, C.B. Sommers, Phys. Rev. B 28 (1983) 1745-1755.

[26] E. Şaşioğlu, L.M. Sandratskii, P. Bruno, Phys. Rev. B 77 (2008) 064417.

[27] C. V Stager, C.C.M. Campbell, Can. J. Phys. 56 (1978) 674-677.

[28] P. Entel, M. Siewert, M.E. Gruner, H.C. Herper, D. Comtesse, R. Arróyave, N. Singh, A. Talapatra, V. V. Sokolovskiy, V.D. Buchelnikov, F. Albertini, L. Righi, V.A. Chernenko, Eur. Phys. J. B 86 (2013) 1-11.

[29] E. Şaşioğlu, L.M. Sandratskii, P. Bruno, Phys. Rev. B 70 (2004) 024427.

[30] P. Entel, M. E. Gruner, S. Fähler, M. Acet, A. Çakır, R. Arróyave, S. Sahoo, T. C. Duong, A. Talapatra, L. Sandratskii, S. Mankowsky, T. Gottschall, O. Gutfleisch, P. Lázpita, V. A. Chernenko, J. M. Barandiaran, V. V. Sokolovskiy, V. D. Buchelnikov, Physica Status Solidi B 255 (2018) 1700296.

[31] E. Şaşıoğlu, L. M. Sandratskii P Bruno, J. Phys.: Condens. Matter 17 (2005) 995.

[32] P. Entel, A. Dannenberg, M. Siewert, H. C. Herper, M. E. Gruner, V. D. Buchelnikov, V. A. Chernenko, Materials Science Forum, 684 (2011) 1-29.